Molecular Cancer Therapeutics

TDP1 is Critical for the Repair of DNA Breaks Induced by Sapacitabine, a Nucleoside also Targeting ATM- and BRCA-Deficient Tumors

Muthana Al Abo[1], Hiroyuki Sasanuma[2], Xiaojun Liu[3], Vinodh N. Rajapakse[1], Shar-yin Huang[1], Evgeny Kiselev[1], Shunichi Takeda[2], William Plunkett[3], and Yves Pommier[1]

Abstract

2'-C-cyano-2'-deoxy-1-β-D-arabino-pentofuranosylcytosine (CNDAC) is the active metabolite of the anticancer drug, sapacitabine. CNDAC is incorporated into the genome during DNA replication and subsequently undergoes β-elimination that generates single-strand breaks with abnormal 3′-ends. Because tyrosyl-DNA phosphodiesterase 1 (TDP1) selectively hydrolyzes nonphosphorylated 3′-blocking ends, we tested its role in the repair of CNDAC-induced DNA damage. We show that cells lacking TDP1 (avian *TDP1*$^{-/-}$ DT40 cells and human *TDP1 KO* TSCER2 and HCT116 cells) exhibit marked hypersensitivity to CNDAC. We also identified BRCA1, FANCD2, and PCNA in the DNA repair pathways to CNDAC. Comparing CNDAC with the chemically related arabinosyl nucleoside analog, cytosine arabinoside (cytarabine, AraC) and the topoisomerase I inhibitor camptothecin (CPT), which both generate 3′-end blocking DNA lesions that are also repaired by TDP1, we found that inactivation of BRCA2 renders cells hypersensitive to CNDAC and CPT but not to AraC. By contrast, cells lacking PARP1 were only hypersensitive to CPT but not to CNDAC or AraC. Examination of *TDP1* expression in the cancer cell line databases (CCLE, GDSC, NCI-60) and human cancers (TCGA) revealed a broad range of expression of *TDP1*, which was correlated with PARP1 expression, *TDP1* gene copy number and promoter methylation. Thus, this study identifies the importance of TDP1 as a novel determinant of response to CNDAC across various cancer types (especially non–small cell lung cancers), and demonstrates the differential involvement of BRCA2, PARP1, and TDP1 in the cellular responses to CNDAC, AraC, and CPT. *Mol Cancer Ther; 16(11); 2543–51. ©2017 AACR.*

Introduction

Sapacitabine is an oral prodrug of the nucleoside analog 2′-C-cyano-2′-deoxy-1-β-D-arabino-pentofuranosylcytosine (CNDAC; Fig. 1A; ref. 1), which is currently in clinical trial for relapsed acute myeloid leukemias (AML) and myelodysplastic syndromes (MDS; ref. 2). The inhibitory activity of CNDAC toward tumor proliferation is achieved by generation of lethal DNA breaks (1, 3). Like its analog cytosine arabinoside (cytarabine, AraC; Fig. 1B), CNDAC is incorporated into DNA during replication (ref. 4; Fig. 1C). Contrary to AraC, CNDAC incorporation does not result in immediate termination of replication fork progression as the cyano substitution does not arrest DNA chain elongation. CNDAC incorporation, however, interferes with the next round of replication (3). Following its incorporation, CNDAC undergoes β-elimination driven by the electron-withdrawing nature of the cyano group in the sugar moiety of CNDAC, leading to the cleavage of the 3′-phosphodiester linkage between CNDAC and the next nucleotide with rearrangement of the terminal CNDAC nucleotide to form 2′-C-cyano-2′,3′-didehydro-2′,3′-dideoxycytidine (CNddC; Fig. 1C; ref. 4). Unless the 3′-blocking lesion is removed and the DNA repaired before the second round of replication, the replication machinery encounters the single-stranded DNA (ssDNA) break (SSB) at the site of CNDAC incorporation (Fig. 1D), and converts the SSB into a lethal double-stranded DNA (dsDNA) break (DSB; refs. 3, 4).

Cells utilize two major pathways for DSB repair: homologous recombination (HR) and nonhomologous end-joining. Previous studies reported that deficiency in HR, but not in nonhomologous end-joining, results in hypersensitivity to CNDAC (3). To perform HR and error free repair, cells use the homologous DNA template present during the S and G_2 phases. During the early steps of HR, 5′-ends of broken dsDNA are resected to generate 3′-overhangs that invades the template DNA. Following which, DNA polymerases extend the ssDNA from the 3′-overhang (5). Thus, noncanonical modifications at the 3′-end of the invading ssDNA inhibit DNA polymerization, completion of DNA repair, and recovery of blocked replication forks.

Tyrosyl–DNA phosphodiesterase 1 (TDP1) was discovered as the enzyme hydrolyzing the phosphodiester bond between a

[1]Developmental Therapeutics Branch and Laboratory of Molecular Pharmacology, Center for Cancer Research, NCI, NIH, Bethesda, Maryland. [2]Department of Radiation Genetics, Kyoto University, Graduate School of Medicine, Yoshida Konoe, Sakyo-ku, Kyoto, Japan. [3]Department of Experimental Therapeutics, University of Texas M.D. Anderson Cancer Center, Houston, Texas.

Note: Supplementary data for this article are available at Molecular Cancer Therapeutics Online (http://mct.aacrjournals.org/).

Corresponding Author: Yves Pommier, National Cancer Institute, Building 37, Room 5068, MD 20892-4255. Phone: 240-760-6142; Fax: 240-541-4475; E-mail: pommier@nih.gov

doi: 10.1158/1535-7163.MCT-17-0110

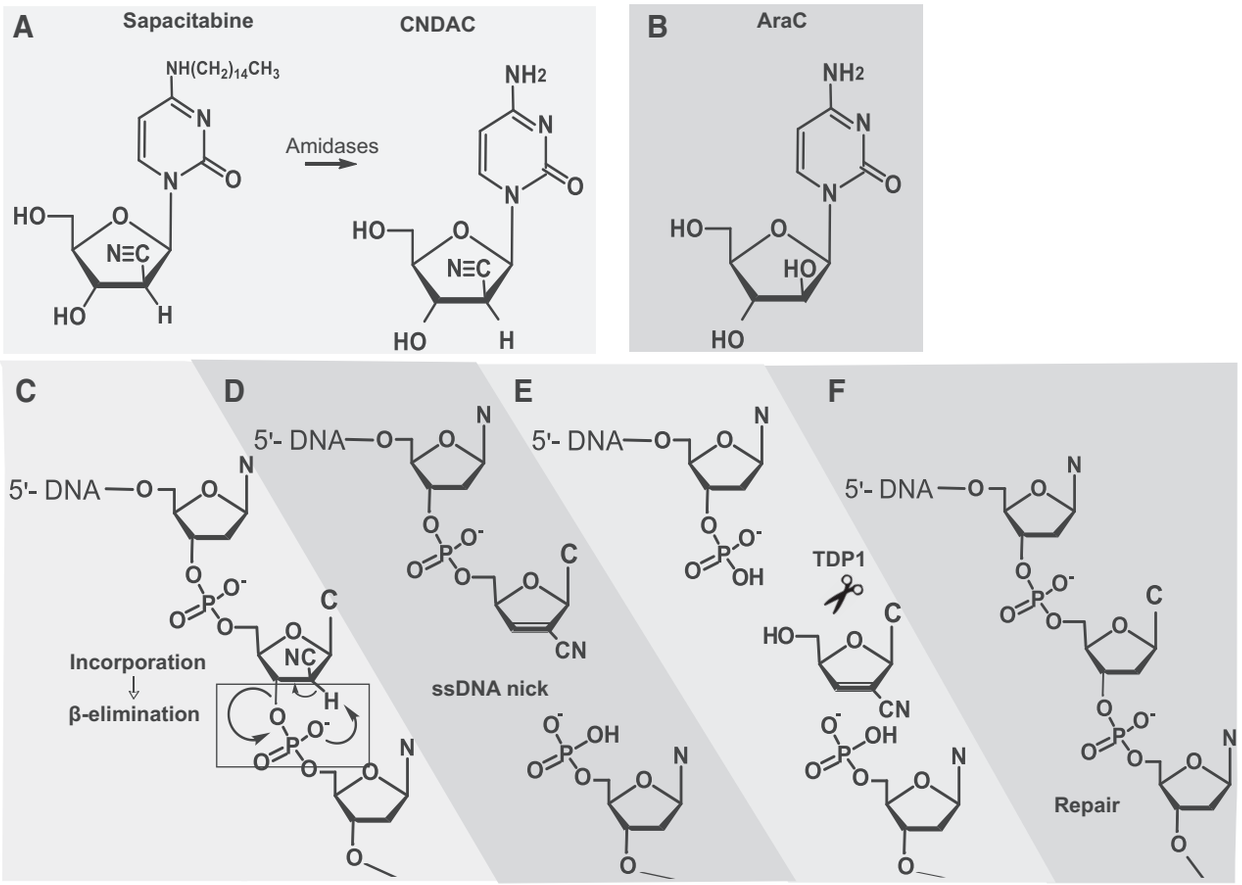

Figure 1.
Illustration of the involvement of TDP1 in the repair of CNDAC-induced DNA damage. **A,** Amidase converts sapacitabine to CNDAC. **B,** Chemical structure of cytosine arabinoside (cytarabine; AraC). **C–D,** Proposed mechanism for the generation of ssDNA nicks by β-elimination of incorporated CNDAC (highlighted in the box). **E,** Excision by TDP1 (shown as scissors) of the 3′-blocking lesion generated by CNDAC. **F,** Repair by gap filing independently of PARP1.

DNA 3′-end and a tyrosyl moiety at the 3′-end of ssDNA that results from trapped topoisomerase I (TOP1; refs. 6–8). Consistently, TDP1$^{-/-}$ cells are hypersensitive to the TOP1 poisoning anticancer drugs, camptothecin (CPT) and its clinical derivatives topotecan and irinotecan (9–12). TDP1 is also critical for the repair of DNA damage induced by chain terminating anticancer and antiviral drugs, such as AraC, acyclovir, zidovudine (AZT) and abacavir (11, 13, 14) and by DNA alkylating agents (11) owing to its 3′-nucleosidase activity (15, 16).

Based on the proposed mechanism of action of CNDAC with formation of a DNA damage intermediate (CNddC) at the 3′-end of a ssDNA break (Fig. 1D), we hypothesized that TDP1 might excise CNDAC-induced 3′-blocking DNA lesions (Fig. 1E and F), and that lack of TDP1 might sensitize cancer cells to CNDAC. To test this hypothesis, we utilized *wild-type* and *TDP1*$^{-/-}$ avian leukemia DT40 cells (11, 13), and generated human *TDP1* knockout TSCER2 and HCT116 cells, and performed viability assays and cell cycle analyses. We also investigated the impact of other DNA repair pathways on the viability of cells treated with CNDAC using our panel of isogenic DT40 cell lines with inactivation of DNA repair pathways (17, 18). Those pathways included repair defects that are known to occur in human cancers such as BRCA1, BRCA2, ATM, Fanconi anemia (FA), and translesion synthesis (TLS) genes. Our results uncover the role of TDP1 in repairing DNA damage induced by sapacitabine and extends our understanding of the common and differential molecular determinants of therapeutics response to sapacitabine, cytarabine and CPT.

Material and Methods

Cell cultures

DT40 cells were cultured at 37°C with 5% CO_2 in RPMI1640 medium supplemented with 1% chicken serum (Life Technologies), 10^{-5} M β-mercaptoethanol, 100 U/mL penicillin, and 100 μg/mL streptomycin, and 10% FBS. Generation of *TDP1*$^{-/-}$ DT40 cells were as previously described in (11). All DT40 mutant cells that are used in this manuscript are the same cells in (17). The human lymphoblastoid cell line, TSCER2 cells (19) were grown in RPMI1640 medium supplemented with 100 μg/mL sodium pyruvate, 100 U/mL penicillin, and 100 μg/mL streptomycin, and 10% FBS and HCT116 cells were grown in DMEM supplemented with 10 FBS. Both TSCER2 and HCT116 were grown at 37°C with 5% CO_2. No authentication was done by the authors.

Generation of TSCER2 *TDP1 KO* cells

To disrupt TDP1 gene, the guide RNA (5′-GCAAAGTTGGATATTGCGTT-3′) was inserted into the pX330 expression vector

(Addgene). For construction of the TDP1 targeting vectors, the left and right arms of the constructs were amplified from genomic DNA, respectively. The left and right arms were amplified using F1/R1 and F2/R2 primers. The resulting fragments were assembled with either *DT-ApA/NEO*^{R} or *DT-ApA/PURO*^{R} (provided from the Laboratory for Animal Resources and Genetic Engineering, Center for Developmental Biology, RIKEN Kobe, http://www.cdb.riken.jp/arg/cassette.html) having been digested with *ApaI* and *AflII* using the GeneArt Seamless Cloning Kit (Invitrogen). Nucleotides indicated by capital letters in F1 and R1 are identical with sequences upstream and downstream, respectively, of the *ApaI* site. Nucleotides indicated by capital letters in in F2 and R2 are identical with sequences upstream and downstream of the *AflII* site. Transfection was done as described previously (20). *TDP1 KO* clones were identified by genomic PCR using F3/R3 (for *NEO*^{R}) and F4/R3 (for *PURO*^{R}). The absence of *TDP1* mRNA was confirmed by RT-PCR using F5/R4 primers (Supplementary Fig. S1A). Expression of GAPDH mRNA as a loading control was amplified by F6/R5.

F1, 5′-GCGAATTGGGTACCGGGCCaaatatcagtttatagagtggcag-3′

R1, 5′-CTGGGCTCGAGGGGGGGCCgaagtcatttatttaaaaa-caact-3′

F2, 5′-TGGGAAGCTTGTCGACTTAAgaacccctcaagcattgtcatttg-3′

R2, 5′-CACTAGTAGGCGCGCCTTAAttggtctcgaactcctgatctcaaa-3′

R3, 5′-GATACTTAATTGGGAAAAGTTCAACTGTAA-3′

F3, 5′-AACCTGCGTGCAATCCATCTTGTTCAATGG-3′

F4, 5′-GTGAGGAAGAGTTCTTGCAGCTCGGTGA-3′

F5, GAAGAAGCCAATCCTGCTTGTGCATGGTGA

R4, TTTGTTTCAGAGAGATCGTGCTTGTGAATG

F6, GCGCCAGTAGAGGCAGGGATGATGT

R5, GCGCCAGTAGAGGCAGGGATGATGT

Generation of HCT116 *TDP1 KO* cells

TDP1 knockout in HCT116 cells were generated by CRISPR genome editing method targeting exon5 of *TDP1* (target site: GTTTAACTACTGCTTTGACGTGG). Plasmid pX330 (21) with the cloned-in target site sequence were cotransfected with a *Puro*-resistance gene flanked by homology arms upstream and downstream of the target site. Transfected cells were selected with 1 μg/mL of puromycin 72 hours post initial transfection for cells with puro-resistance gene recombined into at least one copy of the target site. Established clones from single cell were subsequently screened by biochemical assay (3′-phosphotyrosyl cleavage activity) to identify clones without detectable TDP1 activity (Supplementary Fig. S1A).

Measurement of cellular sensitivity to DNA-damaging drugs

To measure the sensitivity of cells to CNDAC (obtained from Dr. William Plunkett, the University of Texas MD Anderson Cancer Center), AraC (Sigma-Aldrich), or CPT [obtained from the Developmental Therapeutics Program (DCTD, NCI)], 750 DT40 cells were seeded in 96-well white plate (final volume 150 μL/well) from Perkin Elmer Life Sciences with the indicated drugs at 37°C. After 72 hours, cells were assayed in triplicates with the ATPlite 1-Step Kit (PerkinElmer). Briefly, ATPlite solution was added to each well (150 μL for DT40 cells). After 5-minute treatments, luminescence intensity was measured by Envision 2104 Multilabel Reader from Perkin Elmer Life Sciences. Signal intensities of untreated cells were set as 100%.

Cell-cycle analyses

DT40 cells were continuously exposed to fixed concentrations of CNDAC at 37°C for 12 or 24 hours. Harvested cells were fixed with 70% ethanol before re-suspension in PBS containing 50 μg/mL propidium iodide. Samples were then subjected to analysis on an LSRFortessa cell analyzer from BD Biosciences (Franklin Lakes).

TDP1 activity and biochemical assays

The assay was done as described in ref. 22. A 5′-[^{32}P]-labeled ssDNA oligonucleotide containing a 3′-phosphotyrosine (N14Y, 5′-GATCTAAAAGACTT**Y**, Midland Certified Reagents Company) was incubated at 1 nmol/L with whole cell extract for 15 minutes at room temperature in buffer containing 50 mmol/L Tris HCl, pH 7.5, 80 mmol/L KCl, 2 mmol/L EDTA, 1 mmol/L DTT, 40 μg/mL BSA, and 0.01% Tween-20. Reactions were terminated by the addition of 1 volume of gel loading buffer [99.5% (v/v) formamide, 5 mmol/L EDTA, 0.01% (w/v) xylene cyanol, and 0.01% (w/v) bromophenol blue]. Samples were subjected to a 16% denaturing PAGE. Gels were dried and exposed to a PhosphorImager screen (GE Healthcare). Gel images were scanned using a Typhoon FLA 9500 (GE Healthcare).

Colony survival assay

To perform survival assay using TSCER2 cells, we seeded 75 cells in each well of six-well plate in methylcellulose medium with or without CNDAC drug. We prepared the methylcellulose medium as described in ref. 23. After incubating the cells for 12 days at 37°C with 5% CO_2, we counted the number of colonies in each well. To perform survival assay using HCT116 cells, cells were incubated in DMEM medium and next day (after cells adhered to the plate) the medium was aspirated and new media with or without CNDAC were added to the cell. After 15-day incubation, the medium was removed and colonies were fixed on the plate with methanol for 5 minutes. The methanol was removed and the colonies were rinsed with PBS and then stained for 10 minutes with 0.5% crystal violet in water. After the removal of the crystal violet solution, cells were washed again with PBS and left to dry. The number of colonies in each well was counted. To calculate the survival ratios, we divided the number of colonies in wells with CNDAC drugs by the number of colonies in wells which contain medium only.

TOP1 cleavage complex detection by immuno complex of enzyme bioassay

ICE bioassay was performed as described (24, 25). Briefly, Pellet of 2×10^6 TSCER2 cells were lysed in 2 mL 1% Sarkosyl. Cell lysates were added on the top of 1.82, 1.72, 1.50, and 1.45 densities of CsCl solutions. After centrifuging the tubes at 30,700 rpm at room temperature for 20 hours, 1 mL fractions were collected from the bottom of the tubes. One hundred microliters of each fraction were mixed with 100 μL of 25 mmol/L sodium phosphate buffer. Using a slot-blot vacuum, each fraction solutions were blotted onto millipore PVDF membranes. To detect TOP1cleavage complex (TOP1cc), 5% milk in PBS for 1 hour at RT was used for blocking, which was followed by incubation for 2 hours at room temperature with 5% milk containing TOP1 antibody (#556597; BD Biosciences; 1:1,000 dilution). Membrane was washed with PBST (PBS, Tween-20 0.05%) three times for 5 minutes. Horseradish peroxidase–conjugated goat anti-mouse (1:5,000 dilution) antibody (Amersham Biosciences) in 1% milk in PBS was added to the membrane and

incubated for 1 hour at RT. After washing the membrane with PBST five times for 5 minutes, TOP1 was detected by Enhanced Chemiluminescence Detection Kit (Thermo Scientific).

Genomic and bioinformatics analyses

Genomic analyses were performed using rCellMiner (26) based on the genomic databases from the 1,000 cancer cell line of the Cancer Cell Line Encyclopedia (CCLE; http://www.broadinstitute.org/ccle/; ref. 27) and the Genomics of Drug Sensitivity in Cancer (GDSC; http://www.cancerrxgene.org/; ref. 28).

Results

TDP1$^{-/-}$ cells are hypersensitive to CNDAC

To examine the potential impact of TDP1 gene deletion on cell survival, we treated TDP1 proficient (wild-type) and TDP1 deficient (*TDP1*$^{-/-}$) chicken DT40 cells for 72 hours with increasing concentrations of CNDAC and measured cell viability. Elimination of *TDP1* (*TDP1*$^{-/-}$) severely reduced cell viability (IC_{90} was 31 nmol/L in *TDP1*$^{-/-}$ vs. 138 nmol/L in wild-type cells; Fig. 2A). To further establish the causality between TDP1 expression and CNDAC activity, we tested whether human TDP1 (hTDP1) can rescue the hypersensitivity phenotype of *TDP1*$^{-/-}$ cells. Accordingly, expression of human TDP1 (hTDP1) in the *TDP1*$^{-/-}$ cells enhanced cell viability (Fig. 2A). The partial complementation by human TDP1 could be due to species differences.

To further understand the differential effects of CNDAC in TDP1-proficient and deficient cells, we used cell sorting (FACS) to measure cell-cycle distribution and DNA content of CNDAC-treated and untreated cells. When DNA damage overwhelms the cell repair capacity, apoptosis ensues, which is indicated by genomic DNA fragmentation. Therefore, by measuring DNA content while performing cell-cycle analysis, we could estimate the apoptotic fraction (29). Because CNDAC causes DSBs during the second round of replication, analyses were performed after 24 hours, which represents three rounds of replication for the fast growing DT40 cells. A significant fraction of apoptotic cells (28%) appeared as sub-G1 population in the *TDP1*$^{-/-}$ cells treated with CNDAC (Fig. 2B and C). In contrast, sub-G1 populations of wild-type cells were comparable between treated and untreated cells and the *TDP1*$^{-/-}$+hTDP1 cells showed significantly less sub-G1 fraction (16.4%) compared to *TDP1*$^{-/-}$ cells (Fig. 2B and C). We also observed accumulation of G2 fraction with CNDAC treatment, which represents DNA-damaged cells during S-phase. When we treated the cells with lower concentrations of CNDAC for only 12 hours, cell-cycle analysis showed G_2 accumulation

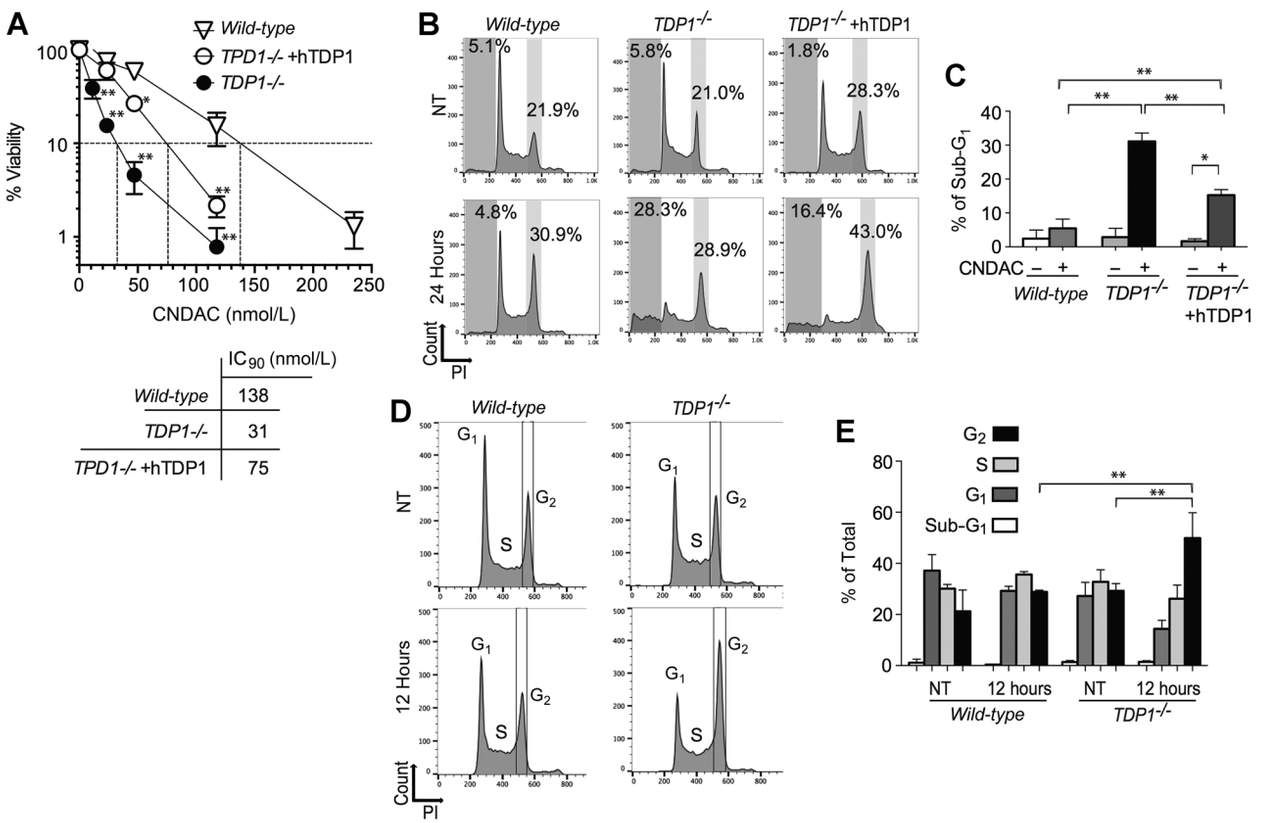

Figure 2.

Hypersensitivity of *TDP1*$^{-/-}$ cells to CNDAC and rescue by human TDP1. **A,** Percent viability (y-axis) of *wild-type* and *TDP1*$^{-/-}$ cells after 72-hour treatment with the indicated concentrations of CNDAC (x-axis). The CNDAC IC_{90} is shown. Representative cell-cycle analysis of *wild-type*, *TDP1*$^{-/-}$, and *TDP1*$^{-/-}$ +hTDP1 cells without treatment (NT), or after 0.47 μmol/L (**B**) or 0.11 μmol/L (**D**) CNDAC for 24 hours. DNA content was measured by propidium iodide (PI). The percentage of sub-G_1 fraction that represents the apoptotic cell fraction is shown. **C, E,** Quantitation of experiments performed as shown in **B** and **D**, respectively. Error bars show the SD of three independent experiments. *T* test (*, $P < 0.05$; **, $P < 0.001$).

(Fig. 2D and E), reflecting replicative DNA damage induced by CNDAC.

Taken together, the cell viabilities and FACS analyses experiments demonstrate that deletion of TDP1 renders cells hypersensitive to CNDAC, implying the role of TDP1 in the repair of CNDAC-induced DNA damage.

CRISPR *TDP1* knockout human TSCER2 lymphoblastoid and HCT116 colon carcinoma cells are hypersensitive to CNDAC

To confirm our findings in human cells, we knocked out the TDP1 gene in human lymphoblastoid TSCER2 and colon carcinoma HCT116 cells using CRISPR-cas9 (Supplementary Fig. S1A and S1B). We validated the efficient knockout of *TDP1* by performing biochemical TDP1 assays in cellular extracts from parental cells (*wild-type*) or *TDP1* knockout (*TDP1* KO) cells (Fig. 3A and B; ref. 11). Next, the cytotoxicity of CNDAC was evaluated in the TSCER2 and HCT116 *TDP1 KO* cells in comparison to the matching parental *wild-type* cells. Colony survival assays using media containing increasing concentration of CNDAC showed that *TDP1 KO* cells were significantly more sensitive than the *wild-type* cells (Fig. 3C and D). These results establish the importance of TDP1 for the repair of CNDAC-induced DNA damage and in the tolerance to CNDAC treatment in human cells.

It has been established that DNA nicks can trap TOP1 and result in TOP1-DNA cleavage complexes (TOP1cc) (30, 31). To answer the question whether the hypersensitivity of *TDP1 KO* could be caused by the ability of CNDAC to trap TOP1cc, we performed ICE bioassays to detect TOP1cc after CNDAC treatment. Repeated experiments failed to detect TOP1cc after CNDAC treatment under conditions where CPT, which was used as positive control, induced signal for TOP1cc (Fig. 3E). The results of these experiments favor the model shown in Figure 1, in which TDP1 repairs CNDAC-induced nicks by its 3′-end nucleosidase activity.

Deletions of BRCA1, BRCA2, FANCD2, or ATM sensitize cells to CNDAC

To uncover additional repair factors/pathways involved in CNDAC-induced DNA damage, we took a genetic approach using our library of DT40 cells that are deficient in various DNA repair pathways (17, 18), including HR, nonhomologous end-joining (NHEJ), FA, and translesion DNA synthesis (TLS) using the DNA polymerase mutant cofactor PCNAK164 (ubiquitin site mutant).

In agreement with recent reports (1, 3), we observed hypersensitivity in *BRCA2*, *ATM*, and *XRCC3* knockout cells (Fig. 4B).

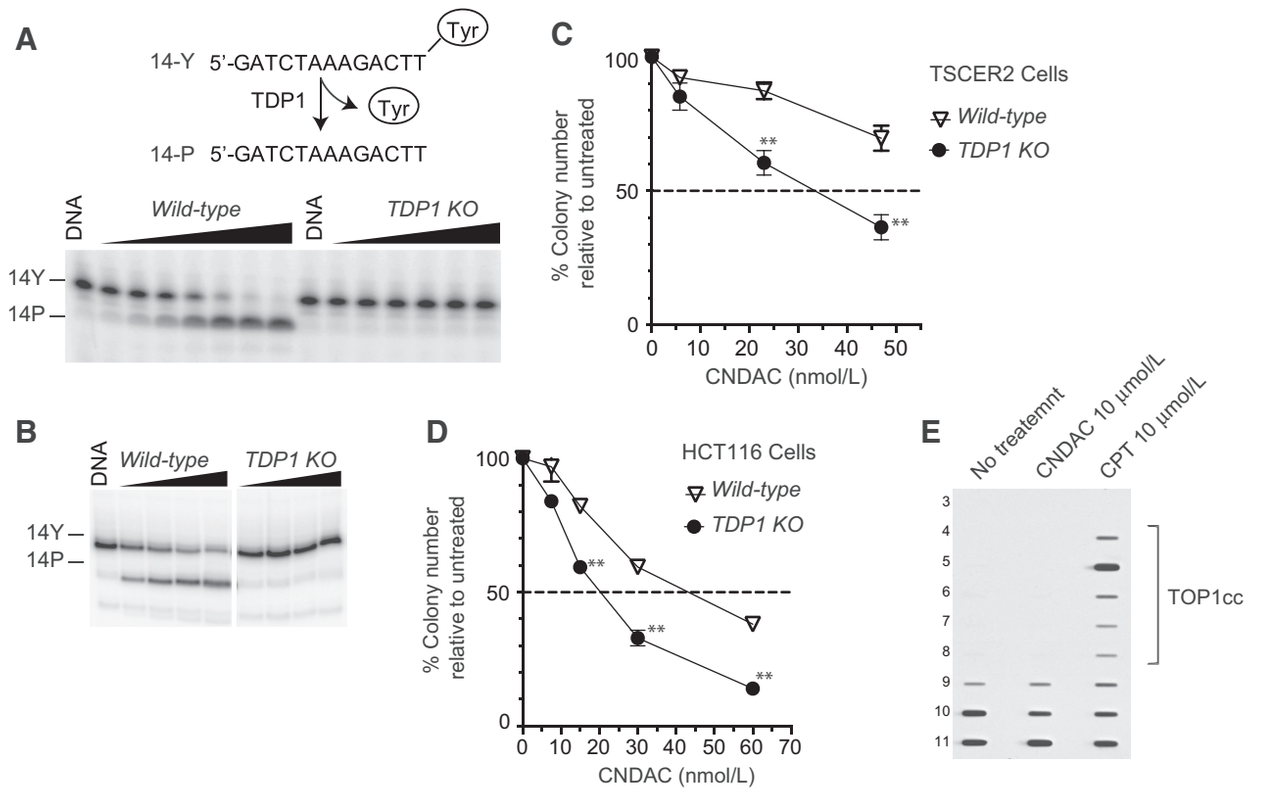

Figure 3.

Human *TDP1* knockout (*TDP1 KO*) TSCER2 and HCT116 cells are hypersensitive to CNDAC. **A** and **B,** Representative biochemical assay showing lack of TDP1 activity in the *TDP1 KO* cells. The reaction scheme is shown at the top (Tyr = 3′-phosphotyrosine). Cellular extracts from either *wild-type* or *TDP1 KO* TSCER2 (**A**) or HCT116 (**B**) cells were tested with serial dilutions (1.6, 5, 14.8, 44.4, 133, 400, and 1,200 μg/mL) for 30 minutes at 25°C. Reduced survival of the TDP1 KO TSCER2 (**C**) and HCT116 (**D**) cells treated with CNDAC. y-axis represents colony numbers relative to untreated cells. Cells were incubated continuously for 12 days with the indicated concentrations of CNDAC (x-axis). Error bars show SD for three independent experiments. *T*-test (**, $P < 0.001$). **E,** Immuno complex of enzyme (ICE) bioassay showing lack of TOP1cc after treatment with 10 μmol/L CNDAC for 3 hours. Ten μmol/L CPT for 3 hours was used as positive control (see Supplementary Fig. S1 for generation of the *TDP1* knockout cell lines). Fractions 3 to 11 of total 12 fractions are shown.

We also observed hypersensitivity in *BRCA1*, *FANCD2* knockout, and *PCNA (PCNA-/K164R)* mutant cells (Fig. 4A and B). By contrast, XRCC6 (Ku70) deficient cells showed no hypersensitivity to CNDAC (Fig. 4B). These results are consistent with replication damage induction by CNDAC and with their repair by HR rather than end-joining. Although TDP1 has been reported to function in association with PARP1 (32), *PARP1* knockout cells were not hypersensitive to CNDAC. This result indicates that TDP1 functions independently of PARP in the repair of CNDAC-induced damage. This is notably different from the reported PARP1-TDP1 coupling for the repair of TOP1-induced DNA damage (32, 33).

Differential roles of TDP1, PARP1 and BRCA2 for the repair of 3′-end DNA lesions induced by CNDAC, AraC and CPT

In addition to CNDAC, TDP1 has been shown to excise a broad range of 3′-end blocking lesions (11, 13, 15, 16, 34) including the chain terminator nucleoside analog AraC and the TOP1 poison CPT, which both generate 3′-end lesions but with different biochemical characteristics. To determine the common and differential repair pathways associated with TDP1, we compared the involvement of PARP1 and BRCA2 in the cellular responses to AraC and CPT in parallel with CNDAC. Figure 5 demonstrates notable differences. Consistent with previous reports, *TDP1* knockout cells are hypersensitive to both AraC and CPT (9, 10, 13) in addition to being hypersensitive to CNDAC, consistent with the broad role of TDP1 in the cleansing of 3′-end blocking lesions. Regarding BRCA2, Figure 5 shows that *BRCA2* knockout cells are hypersensitive to CNDAC and CPT but not to AraC. These results are consistent with the conclusion that the DNA lesions generated by CNDAC and CPT are DSBs in S-phase, which are repaired by HR. They also demonstrate that AraC-induced damage is not repaired via HR. In addition, while *PARP1* knockout cells are hypersensitive to CPT (35), they are not hypersensitive to CNDAC or AraC (Fig. 5). This result shows that TDP1 can function independently of PARP1 in response to CNDAC- or AraC-induced DNA damages. Our findings highlight the differential cellular responses to 3′-end blocking anticancer drugs and the involvement of different repair factors and pathways.

TDP1 expression range in cancer cell lines and in cancer samples from the TCGA

Because of the emerging importance of TDP1 as a potential determinant of response to an increasing number of therapeutically relevant DNA damaging agents, we examined TDP1 expression in publicly available cancer genomic databases.

In the 1,000 cancer cell line databases of the CCLE (27) and the GDSC (28) projects, *TDP1* expression varies broadly across cell lines and tissues of origin (Fig. 6A–D y-axis and Supplementary Fig. S2A). This variation is due, in part to amplifications and deletions (copy number variation, CNV) of the *TDP1* gene locus (Fig. 6A-C) on chromosome 14q32.11. Moreover, leukemia and blood cancers tend to have high *TDP1* expression (Fig. 6B) while non-small cell lung cancers (NSCLC) have the broadest *TDP1* expression range with some cells having background (no significant) *TDP1* expression (Fig. 6C; Supplementary Fig. S2A). In the NSCLC cell lines, we found that lack of *TDP1* expression is also driven by promoter hypermethylation (Fig. 6D) (36).

Similarly, in The Cancer Genome Atlas (TCGA) database, *TDP1* expression varies widely (Fig. 6E; Supplementary Fig. S2B), and the NSCLC samples show the broadest *TDP1* expression range with some cancers having insignificant *TDP1* mRNA (Fig. 6E). By contrast, acute myelocytic leukemia (AML) samples show consistently high *TDP1* expression (Fig. 6E; Supplementary Fig. S2B). Together, these genomic analyses demonstrate that *TDP1* exhibits a wide range of expression, most notably in NSCLC, and that *TDP1* expression variation correlates positively with *TDP1* gene CNV (Fig. 6A–C) and negatively with *TDP1* promoter methylation (Fig. 6D).

Discussion

Here we report evidence supporting that *TDP1* repairs the DNA damage induced by CNDAC, the active metabolite of the novel anticancer drug sapacitabine, which supports the proposed mechanism of DNA damage by sapacitabine (Fig. 1). We show that the avian leukemia *TDP1* knockout DT40 cells are almost as hypersensitive as BRCA1- or BRCA2-deficient cells to CNDAC compared to wild-type cells (Figs. 2 and 4), and that they are similarly hypersensitive as cells defective for ATM or FANCD2 (Fig. 4). We also expand these findings by showing that human TSCER2 lymphoblastoid and HCT116 colon carcinoma *TDP1* knockout cells are hypersensitive to CNDAC as well (Fig. 3), and that complementation of DT40 *TDP1* knockout cells with human *TDP1* rescues the viability of those cells in response to CNDAC (Figs. 1 and 2).

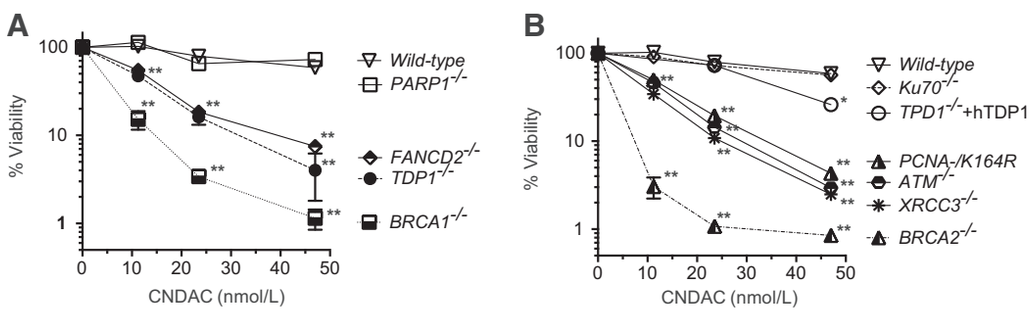

Figure 4.

Hypersensitivity of isogenic DNA repair defective DT40 cells to CNDAC. **A** and **B**, Viability assays were performed as described in Figure 2. Error bars represent SD of at least three independent determinations. Error bars are not visible when they are encompassed within the size of the symbols. *T* test (*, $P < 0.05$; **, $P < 0.001$). Viability curves are split in two panels (A and B) for clarity.

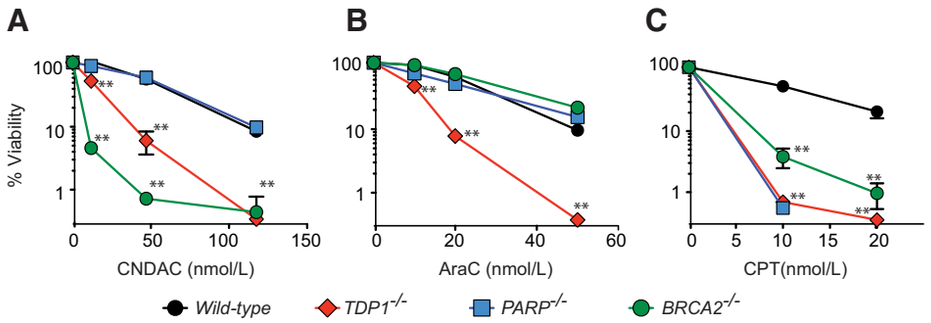

Figure 5.
Differential impact of TDP1, PARP, and BRCA2 loss against representative 3′-end ssDNA lesions. The viability of the indicated DNA repair mutants DT40 cells after treatment with CNDAC (**A**), AraC (**B**), or CPT (**C**) was performed as described in Figure 1. *T* test (**, $P < 0.001$).

The mode of action of widely used anticancer nucleoside analogs, such as cytarabine, is to block replication by incorporating a modified nucleotide at the 3′-end of DNA during replication chain elongation. Previous results (11, 13) as well as results shown here demonstrate that TDP1 plays a critical role in processing these abnormal 3′-ends, which ultimately enables the repair process. Although the 3′-end blocking anticancer drugs tested here generate 3′-end lesions that require TDP1 (Fig. 5), additional repair pathways downstream to TDP1 vary. Indeed, we observed differential requirement of BRCA2 and PARP1 for CNDAC, CPT, or AraC. This is likely due to the fact that these agents cause DNA lesions that relate to replication in different ways: (i) CNDAC and CPT damage the DNA template, whereas AraC damages the newly synthesized DNA; (ii) CPT blocks replication ahead of replication forks, whereas AraC terminates the elongation of replication forks and CNDAC stops replication by breaking the template; (iii) CPT and CNDAC cause replication-mediated double-stranded DNA breaks, which is not the case for AraC; and (iv) CNDAC induces ssDNA nicks only behind the replication fork, whereas CPT generates TOP1 cleavage complexes ahead of replication forks.

Recently, using Chinese hamster cells, it was reported that the combination of CNDAC with PARP1 inhibitors, olaparib,

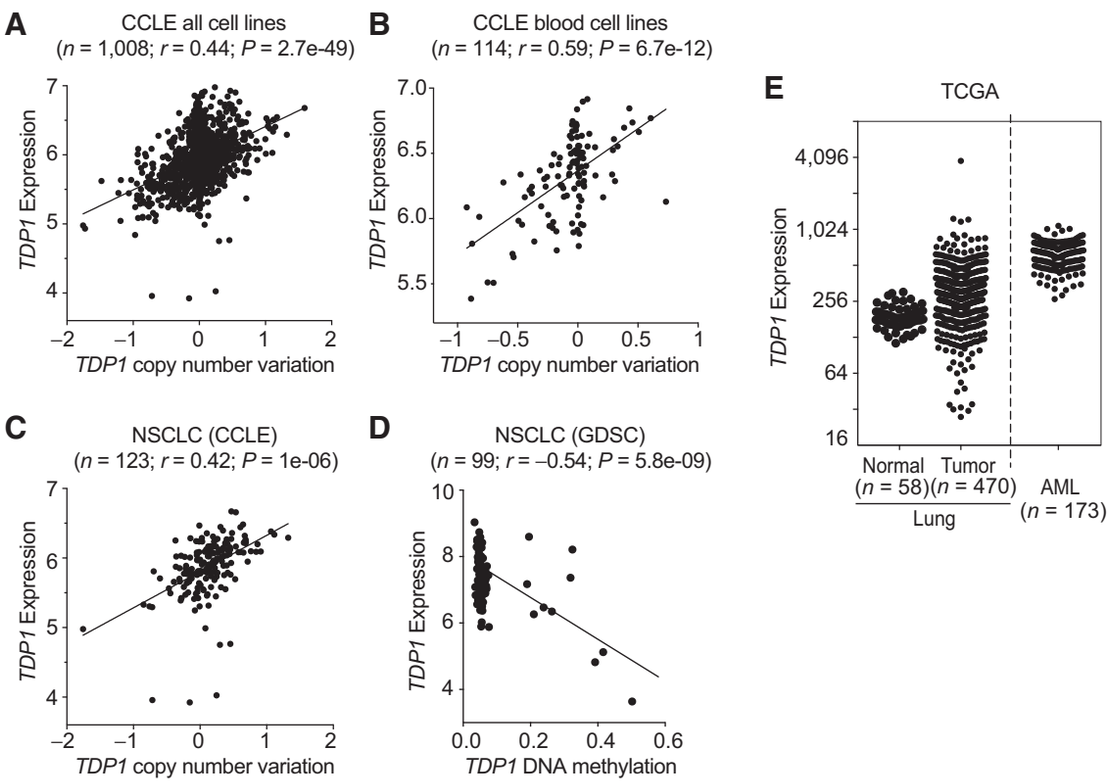

Figure 6.
TDP1 expression varies among cancer cells of the same tissue of origin as well as among cancer cells from different tissues of origin. *TDP1* mRNA (y-axis, values represent log 2 values for panels **A–D**) in relation to CNV (x-axis) in the overall collection of CCLE cancer cell lines (**A**) in the CCLE blood cancer cell lines (**B**), and in the non–small cell lung cancer cell lines (NSCLC), of the CCLE (**C**). **D**, *TDP1* expression (*y*-axis) and methylation of the *TDP1* promoter (x-axis) in the NSCLC cell lines from the GDSC database. **E,** Comparison of *TDP1* expression determined by RNA-Seq (RSEM) in normal lung cells vs. NSCLC cells and acute myeloid leukemia (AML) cells (see Supplementary Fig. S2).

rucaparib, and talazoparib was synergistic in HR-deficient (BRCA2-, XRCC3-, and RAD51D-deficient cells) but not in wild-type cells at relatively low concentrations (37). Our results showing no impact of PARP inactivation on CNDAC cytotoxicity in wild-type cells are consistent with this previous report.

Understanding the specific repair pathways for new drugs is critical for their effective development and precise use as anticancer agents. It is notable that the pathways that repair sapacitabine-induced DNA damage (BRCA1, BRCA2, ATM, and FA) have been found defective in a significant number of cancers, suggesting they could be used for synthetic lethality approaches. Scoring TDP1 deficiency in cancers could be included in the screening of tumors in addition to ATM, HR, and FA genes mutations for choosing sapacitabine as a therapeutic option beyond leukemia and myelodysplastic syndromes.

In this study, we extend our initial finding that TDP1 is inactivated in two of the lung cancer cell lines of the NCI-60 (36) by showing lowest TDP1 expression in NSCLC cancer cell lines and tumor samples, and establishing that both gene copy number defects and promoter hypermethylation cause such defective expression. We also found a broad range of expression of *TDP1* across cancer cells (Fig. 6 and Supplementary Fig. S2). Further analyses (26) in the 1,000 cell line collections [CCLE (27) and GDSC (28)] show that *TDP1* expression is highly significantly correlated with other DNA repair genes including *PARP1*, *BRCA2*, *BRCA1*, *FANCM*, and *BLM* and DNA replication genes including *POLD1*, *POLE2*, and *ORC1*, suggesting the coordinated activation of the DNA repair and replication pathways in cancer cells.

Disclosure of Potential Conflicts of Interest

No potential conflicts of interest were disclosed.

Authors' Contributions

Conception and design: M. Al Abo, W. Plunkett, Y. Pommier
Development of methodology: M. Al Abo, Y. Pommier
Acquisition of data (provided animals, acquired and managed patients, provided facilities, etc.): M. Al Abo, S.N. Huang, E. Kiselev
Analysis and interpretation of data (e.g., statistical analysis, biostatistics, computational analysis): M. Al Abo, H. Sasanuma, V.N. Rajapakse, Y. Pommier
Writing, review, and/or revision of the manuscript: M. Al Abo, X. Liu, E. Kiselev, W. Plunkett, Y. Pommier
Administrative, technical, or material support (i.e., reporting or organizing data, constructing databases): M. Al Abo, S. Takeda, Y. Pommier
Study supervision: Y. Pommier

Grant Support

Our studies are supported by the Intramural Program of the National Cancer Institute, Center for Cancer Research (Z01 BC006150) to Y. Pommier and M. Al Abo; NIH-NCI (R01 CA028596) to W. Plunkett and X. Liu; and a Grant-in-Aid from the Ministry of Education, Science, Sport and Culture to S. Takeda (KAKENHI 16H06306), and H. Sasanuma (KAKENHI 16H02953)

The costs of publication of this article were defrayed in part by the payment of page charges. This article must therefore be hereby marked *advertisement* in accordance with 18 U.S.C. Section 1734 solely to indicate this fact.

Received February 1, 2017; revised May 24, 2017; accepted July 27, 2017; published OnlineFirst August 11, 2017.

References

1. Liu XJ, Nowak B, Wang YQ, Plunkett W. Sapacitabine, the prodrug of CNDAC, is a nucleoside analog with a unique action mechanism of inducing DNA strand breaks. Chin J Cancer 2012; 31:373–80.
2. Kantarjian H, Garcia-Manero G, O'Brien S, Faderl S, Ravandi F, Westwood R, et al. Phase I clinical and pharmacokinetic study of oral sapacitabine in patients with acute leukemia and myelodysplastic syndrome. J Clin Oncol 2010;28:285–91.
3. Liu X, Wang Y, Benaissa S, Matsuda A, Kantarjian H, Estrov Z, et al. Homologous recombination as a resistance mechanism to replication-induced double-strand breaks caused by the antileukemia agent CNDAC. Blood 2010;116:1737–46.
4. Azuma A, Huang P, Matsuda A, Plunkett W. 2'-C-cyano-2'-deoxy-1-beta-D-arabino-pentofuranosylcytosine: a novel anticancer nucleoside analog that causes both DNA strand breaks and G(2) arrest. Mol Pharmacol 2001;59:725–31.
5. Krejci L, Altmannova V, Spirek M, Zhao X. Homologous recombination and its regulation. Nucleic Acids Res 2012;40:5795–818.
6. Dexheimer TS, Stephen AG, Fivash MJ, Fisher RJ, Pommier Y. The DNA binding and 3'-end preferential activity of human tyrosyl-DNA phosphodiesterase. Nucleic Acids Res 2010;38:2444–52.
7. Pouliot JJ, Yao KC, Robertson CA, Nash HA. Yeast gene for a Tyr-DNA phosphodiesterase that repairs topoisomerase I complexes. Science 1999;286:552–5.
8. Liu C, Pouliot JJ, Nash HA. Repair of topoisomerase I covalent complexes in the absence of the tyrosyl-DNA phosphodiesterase Tdp1. Proc Natl Acad Sci U S A 2002;99:14970–5.
9. El-Khamisy SF, Saifi GM, Weinfeld M, Johansson F, Helleday T, Lupski JR, et al. Defective DNA single-strand break repair in spinocerebellar ataxia with axonal neuropathy-1. Nature 2005;434:108–13.
10. Miao ZH, Agama K, Sordet O, Povirk L, Kohn KW, Pommier Y. Hereditary ataxia SCAN1 cells are defective for the repair of transcription-dependent topoisomerase I cleavage complexes. DNA Repair 2006;5:1489–94.
11. Murai J, Huang SY, Das BB, Dexheimer TS, Takeda S, Pommier Y. Tyrosyl-DNA phosphodiesterase 1 (TDP1) repairs DNA damage induced by topoisomerases I and II and base alkylation in vertebrate cells. J Biol Chem 2012;287:12848–57.
12. Meisenberg C, Gilbert DC, Chalmers A, Haley V, Gollins S, Ward SE, et al. Clinical and cellular roles for TDP1 and TOP1 in modulating colorectal cancer response to irinotecan. Mol Cancer Ther 2015;14:575–85.
13. Huang SY, Murai J, Dalla Rosa I, Dexheimer TS, Naumova A, Gmeiner WH, et al. TDP1 repairs nuclear and mitochondrial DNA damage induced by chain-terminating anticancer and antiviral nucleoside analogs. Nucleic Acids Res 2013;41:7793–803.
14. Tada K, Kobayashi M, Takiuchi Y, Iwai F, Sakamoto T, Nagata K, et al. Abacavir, an anti-HIV-1 drug, targets TDP1-deficient adult T cell leukemia. Sci Adv 2015;1:e1400203.
15. Interthal H, Chen HJ, Champoux JJ. Human Tdp1 cleaves a broad spectrum of substrates including phosphoamide linkages. J Biol Chem 2005; 280:36518–28.
16. Zhou T, Lee JW, Tatavarthi H, Lupski JR, Valerie K, Povirk LF. Deficiency in 3'-phosphoglycolate processing in human cells with a hereditary mutation in tyrosyl-DNA phosphodiesterase (TDP1). Nucleic Acids Res 2005;33: 289–97.
17. Maede Y, Shimizu H, Fukushima T, Kogame T, Nakamura T, Miki T, et al. Differential and common DNA repair pathways for topoisomerase I- and II-targeted drugs in a genetic DT40 repair cell screen panel. Mol Cancer Ther 2014;13:214–20.
18. Murai J, Huang S-yN, Das BB, Renaud A, Zhang Y, Doroshow JH, et al. Trapping of PARP1 and PARP2 by clinical PARP inhibitors. Cancer Res 2012;72:5588–99.
19. Honma M, Izumi M, Sakuraba M, Tadokoro S, Sakamoto H, Wang W, et al. Deletion, rearrangement, and gene conversion; genetic consequences of chromosomal double-strand breaks in human cells. Environ Mol Mutagen 2003;42:288–98.
20. Hoa NN, Akagawa R, Yamasaki T, Hirota K, Sasa K, Natsume T, et al. Relative contribution of four nucleases, CtIP, Dna2, Exo1 and Mre11, to the

initial step of DNA double-strand break repair by homologous recombination in both the chicken DT40 and human TK6 cell lines. Genes Cells 2015;20:1059–76.
21. Cong L, Ran FA, Cox D, Lin S, Barretto R, Habib N, et al. Multiplex genome engineering using CRISPR/Cas systems. Science 2013;339: 819–23.
22. Das BB, Dexheimer TS, Maddali K, Pommier Y. Role of tyrosyl-DNA phosphodiesterase (TDP1) in mitochondria. Proc Natl Acad Sci U S A 2010;107:19790–5.
23. Tsuda M, Terada K, Ooka M, Kobayashi K, Sasanuma H, Fujisawa R, et al. The dominant role of proofreading exonuclease activity of replicative polymerase epsilon in cellular tolerance to cytarabine (Ara-C). Oncotarget 2017;8:33457–74.
24. Pourquier P, Takebayashi Y, Urasaki Y, Gioffre C, Kohlhagen G, Pommier Y. Induction of topoisomerase I cleavage complexes by 1-beta -D-arabinofuranosylcytosine (ara-C) in vitro and in ara-C-treated cells. Proc Natl Acad Sci U S A 2000;97:1885–90.
25. Subramanian D, Kraut E, Staubus A, Young DC, Muller MT. Analysis of topoisomerase I/DNA complexes in patients administered topotecan. Cancer Res 1995;55:2097–103.
26. Luna A, Rajapakse VN, Sousa FG, Gao J, Schultz N, Varma S, et al. rcellminer: exploring molecular profiles and drug response of the NCI-60 cell lines in R. Bioinformatics 2016;32:1272–4.
27. Barretina J, Caponigro G, Stransky N, Venkatesan K, Margolin AA, Kim S, et al. The Cancer Cell Line Encyclopedia enables predictive modelling of anticancer drug sensitivity. Nature 2012;483: 603–307.
28. Garnett MJ, Edelman EJ, Heidorn SJ, Greenman CD, Dastur A, Lau KW, et al. Systematic identification of genomic markers of drug sensitivity in cancer cells. Nature 2012;483:570–5.
29. Umansky SR, Korol BA, Nelipovich PA. In vivo DNA degradation in thymocytes of gamma-irradiated or hydrocortisone-treated rats. Biochim Biophys Acta 1981;655:9–17.
30. Pourquier P, Pilon A, Kohlhagen G, Mazumder A, Sharma A, Pommier Y. Trapping of mammalian topoisomerase I and recombinations induced by damaged DNA containing nicks or gaps: importance of DNA end phosphorylation and camptothecin effects. J Biol Chem 1997;272:26441–7.
31. Huang SN, Williams JS, Arana ME, Kunkel TA, Pommier Y. Topoisomerase I-mediated cleavage at unrepaired ribonucleotides generates DNA double-strand breaks. EMBO J 2017;36:361–73.
32. Das BB, Huang SY, Murai J, Rehman I, Ame JC, Sengupta S, et al. PARP1-TDP1 coupling for the repair of topoisomerase I-induced DNA damage. Nucleic Acids Res 2014;42:4435–49.
33. Murai J, Marchand C, Shahane SA, Sun H, Huang R, Zhang Y, et al. Identification of novel PARP inhibitors using a cell-based TDP1 inhibitory assay in a quantitative high-throughput screening platform. DNA Repair 2014;21:177–82.
34. Zhou T, Akopiants K, Mohapatra S, Lin PS, Valerie K, Ramsden DA, et al. Tyrosyl-DNA phosphodiesterase and the repair of 3'-phosphoglycolate-terminated DNA double-strand breaks. DNA Repair 2009;8:901–11.
35. Zhang YW, Regairaz M, Seiler JA, Agama KK, Doroshow JH, Pommier Y. Poly(ADP-ribose) polymerase and XPF-ERCC1 participate in distinct pathways for the repair of topoisomerase I-induced DNA damage in mammalian cells. Nucleic Acids Res 2011;39:3607–20.
36. Gao R, Das BB, Chatterjee R, Abaan OD, Agama K, Matuo R, et al. Epigenetic and genetic inactivation of tyrosyl-DNA-phosphodiesterase 1 (TDP1) in human lung cancer cells from the NCI-60 panel. DNA Repair 2014;13:1–9.
37. Liu X, Jiang Y, Nowak B, Hargis S, Plunkett W. Mechanism-based drug combinations with the DNA strand-breaking nucleoside analog CNDAC. Mol Cancer Ther 2016;15:2302–13.